# Rapid and Sensitive Differentiation of Anomers, Linkage, and Position Isomers of Disaccharides Using High-Field Asymmetric Waveform Ion Mobility Spectrometry (FAIMS)

Wojciech Gabryelski and Kenneth L. Froese
Department of Public Health Sciences, University of Alberta, Edmonton, Alberta, Canada

A challenging aspect of structural elucidation of carbohydrates is gaining unambiguous information for anomers, linkage, and position isomers. Such isomers with identical mass can't be easily distinguished in mass spectrometry and a separation step is required prior to mass spectrometry identification. In our laboratory, gas-phase separation and differentiation of anomers, linkage, and position isomers of disaccharides was achieved using High-Field Asymmetric Waveform Ion Mobility Spectrometry (FAIMS). The FAIMS method responds to changes in ion mobility at high field rather than absolute values of ion mobility, and was shown to provide efficient separation and identification of disaccharide isomers at high sensitivity. Separation of analyzed disaccharide isomers can be accomplished at low nM level in a matter of seconds without sample purification or fractionation. Capability for examining a large population of ionic species of disaccharides by this method allowed for correlating structural details of disaccharide isomers with their separation properties in FAIMS. Results for disaccharide isomers indicate that this method could be applied to a larger group of carbohydrates. (J Am Soc Mass Spectrom 2003, 14, 265–277) © 2003 American Society for Mass Spectrometry

Biological functions and chemical properties of carbohydrates and their conjugates with proteins and lipids depend on structural details such as sequence, linkage type, anomeric configuration, and sugar modifications. A variety of analytical methods have been used to characterize these structural features.

Mass spectrometry has shown a unique ability to resolve certain structural ambiguities. Permethylation is a well developed but time-consuming GC-MS method in linkage analysis of oligosaccharides [1, 2]. Other methods implementing the derivatization of saccharides have been used to obtain their structural information [3–11]. The soft mass spectrometry ionization techniques such as fast atom bombardment (FAB) [12–16], liquid secondary ionization mass spectrometry (LSIMS) [17, 18], along with matrix-assisted laser desorption ionization (MALDI) [19–23], and electrospray ionization (ESI) [24–28] have gained attention as approaches to investigate underivatized oligosaccharides. Collision-induced dissociation (CID) offers the possibility to assign details of carbohydrate structure such as sugar sequence for linear oligosaccharides [12], linkage position [12, 15–17, 29], and differentiation of anomers [25, 30]. In addition to analyzing protonated or deprotonated molecular ions of saccharides in CID, alkali metal adduct ions have been used to promote fragmentation of ligand-carbohydrate complexes. In the positive ion mode, calcium and magnesium adducts of oligosaccharides were investigated for the elucidation of the linkage position of trisaccharides [26] and cobalt complexes have been used to differentiate the anomeric configuration of disaccharides [30]. In the negative ion mode, decomposition of chloride adducts was investigated for differentiation of the linkage position of disaccharides [31].

Despite recent advances in tandem mass spectrometry of carbohydrates, the spectral differences for some isomers are very small and they do not provide unambiguous identification. This is especially true when a mixture of isomers with the same *m/z* has to be analyzed. In such applications a separation step is required prior to mass spectrometry identification. Liquid separation methods, such as chromatography and electrophoresis, allow for separation of carbohydrate species. However, the narrow range in polarity of many sugar isomers and their similar size make isomer separation difficult and time-consuming. The extremely

Published online February 6, 2003
Address reprint requests to Dr. W. Gabryelski, Department of Public Health Sciences, University of Alberta, 10-110 Clinical Science Building, Edmonton, Alberta T6G 2G3, Canada. E-mail: wg@ualberta.ca


1044-0305/03/$30.00
doi:10.1016/S1044-0305(03)00002-3

Received September 20, 2002
Revised December 23, 2002
Accepted December 27, 2002

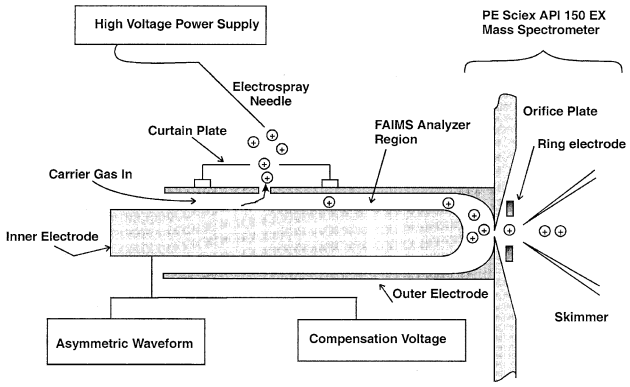


**Figure 1**. Diagram of ESI-FAIMS-MS.

hydrophilic nature of carbohydrates and the absence of electrical charge on carbohydrate molecules require that chromatographic and electrophoretic procedures have to be adapted to carbohydrate analysis with separation conditions incompatible with mass spectrometry detection. In contrast, gas-phase separation methods based on differences in ion mobility of gaseous ions offer a number of advantages over traditional liquid separation methods, including speed and sensitivity of detection. Ion mobility spectrometry (IMS) has been shown to be an effective tool in separating gas-phase isobaric ions [32] but this technique was not extensively used in separation of carbohydrates [33, 34].

In our laboratory, gas-phase separation and isomeric differentiation of isobaric disaccharides was achieved using high-field asymmetric waveform ion mobility spectrometry (FAIMS). The FAIMS method responds to changes in ion mobility at high field rather than absolute values of ion mobility, and provides efficient separation and identification of disaccharide isomers at high sensitivity. Separation of analyzed disaccharides can be accomplished in a few seconds at low nM concentrations without sample purification or fractionation. Experimental requirements for this application are discussed to demonstrate the unique capabilities and liabilities of this new technique. Finally, a model of FAIMS separation of disaccharide isomers is proposed.

## Experimental

### *Instrumentation*

A diagram of the ESI-FAIMS-MS instrument built at PHS Department University of Alberta is shown in Figure 1. The FAIMS analyzer used in this work consisted of the inner electrode (16 mm o.d.) and the outer electrode (20 mm i.d.) so the spacing between the electrodes in cylindrical part of the FAIMS analyzer region was kept constant at 2 mm. The distance between spherical surfaces of the inner and the outer electrode was kept at 2.3 or 2.4 mm. An asymmetric waveform [35] that provided dispersion voltage up to ±3700 V at 750 kHz was applied to the inner cylinder of the FAIMS device along with the DC compensation voltage. The relative amplitude of the sinusoidal wave and its harmonic [36] were approximately 3:1. The electrospray source consisted of a length of fused silica capillary (30 cm × 50 μm i.d. × 180 μm o.d.) that protruded through a stainless steel capillary (10 cm × 200 μm i.d. × 430 μm o.d.). Sample solutions were delivered to this source by a Harvard Apparatus Model 22 syringe pump at a flow rate of 1 μL/min. The stainless steel capillary was kept at a potential of +4000 V in positive ion mode and −3200 V in negative ion mode. The tip of the needle was located approximately 1 cm from the 2 mm opening in the curtain plate and positioned at 45° with respect to the curtain plate. The curtain plate was electrically insulated from the outer cylinder of the FAIMS device and kept at a potential of +1000 V in positive ion mode and −1000 V in negative ion mode. The nitrogen carrier gas was passed through a charcoal/molecular sieve filter and introduced into the FAIMS analyzer region. Before mass detection, ions were transported from the atmospheric pressure region of FAIMS through the 250 μm diameter opening in the orifice plate into the low pressure region of the PE Sciex (Concord, Canada) API 150 EX quadrupole mass spectrometer equipped with the ring electrode assembly and the skimmer.

### *Ion Separation in FAIMS*

The principles of ion separation in FAIMS have been described in detail [37, 38] and are briefly summarized here. In order to separate two ions in FAIMS, the *relative ion mobility* expressed as the ratio of the ion mobility at high electric field to the ion mobility at low electric field has to be different for these two ions. High and low electric field conditions are generated between the cylindrical plates of FAIMS (Figure 1) by application of the asymmetric waveform to the inner cylinder electrode. During one cycle of the waveform, an ion experiences a short duration of high electric field and moves at high-field mobility toward one of the cylinder electrodes. During the same cycle of the waveform, the ion also experiences a longer duration of oppositely directed low electric field and moves with low-field ion mobility toward the opposite cylinder electrode. The waveform is designed in such a way that if the mobility of the ion is the same under high- and low-field conditions, the ion does not experience any displacement from the center in the space between two cylinders. A difference in relative ion mobility at high and low field, however, will result in a constant drift of the ion toward one of the cylindrical electrodes. To transmit the ion through the FAIMS, a DC voltage [compensation voltage (CV)] has to be applied to the inner electrode to compensate for the ion drift and keep the ion of interest focused in the annular space between the electrodes. The ion can be transmitted through FAIMS and sampled by the mass spectrometer only when the appropriate value of the CV is used.

**Table 1.** Disaccharide isomers examined in this study

| | |
|---|---|
| | **Anomers** |
| 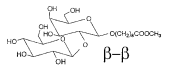 | **[1]** $\beta$DGlc(1-2)$\beta$DGalO$(CH_2)_8COOCH_3$ |
| 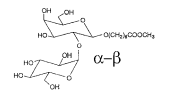 | **[2]** $\alpha$DGlc(1-2)$\beta$DGalO$(CH_2)_8COOCH_3$ |
| | **Linkage isomers** |
| 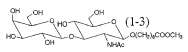 | **[3]** $\beta$DGal(1-3)$\beta$DGlcNHAcO$(CH_2)_8COOCH_3$ |
| 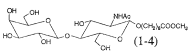 | **[4]** $\beta$DGal(1-4)$\beta$DGlcNHAcO$(CH_2)_8COOCH_3$ |

**Position isomers** of $\beta$DGal(1-4)$\beta$DGlcNHAcO$(CH_2)_7CH_3$ (Nac-Lactose)

|  |  |  |  |
|---|---|---|---|
| **[11]** | **[21]** | **[31]** | **[41]** |
| **[12]** | **[22]** | **[32]** | **[42]** |
| **[13]** | **[23]** | **[33]** | **[43]** |
| **[14]** | **[24]** | **[34]** | **[44]** |
| **[15]** | **[25]** | **[35]** | **[45]** |
| **[16]** | **[26]** | **[36]** | **[46]** |

### *Disaccharide Isomers and Chemicals*

Disaccharide isomers used in FAIMS experiments are presented in Table 1. They include two anomers, two linkage isomers, and position isomers with different derivative groups located at different carbon positions. The disaccharides were kindly provided by Dr. Ole Hindsgaul. If not stated otherwise, 1 $\mu$M solutions of disaccharides in methanol/water (9/1 vol/vol) with 0.2 mM ammonium acetate were analyzed. In the positive mode of ESI, samples were spiked with chloride salts of Li, Na, K, Rb, and Cs at 25 $\mu$M. In negative ion ESI, samples were spiked with ammonia to 0.05% concentration, ammonium chloride, ammonium acetate, and nine haloacetic acids at 25 $\mu$M. Monochloroacetic acid (MCA), trichloroacetic acid (TCA), monobromoacetic acid (MBA), and dibromoacetic acid (DBA) were purchased from Fluka (Buchs, Switzerland). Tribromoacetic acid (TBA), dichloroacetic acid (DCA), bromochloroacetic acid (BCA), raffinose, and melezitose were supplied by Aldrich Chemical Company (Oakville, Canada), while bromodichloroacetic acid (BDCA) and chlorodibromoacetic acid (CDBA) were obtained from Supelco. HPLC-grade methanol and HPLC-grade water, ammomium acetate, ammonium chloride, lithium chloride, sodium chloride, potasium chloride, rubidium chloride, and cesium chloride were purchased from Fisher Scientific Company (Nepean, Canada).

## Results and Discussion

### *MS Detection of Disaccharide Ions Separated by FAIMS in Positive Ion Mode*

Figure 2 shows CV spectra and mass spectra acquired at selected CV settings of ions originating from the $\beta$-D-Glc(1-2)$\beta$-D-GalOR disaccharide **1** in positive ion mode of ESI. The total ion CV spectrum (Figure 2a) was acquired by ramping the CV from 1 to 9 volts at 0.1 V increments and the mass spectrum (30–2000 *m/z*, 0.2 a$\mu$ step size, and 5 ms dwell time) was recorded at each compensation voltage step. This CV spectrum that contains complete mass spectral information similar to that generated by IMS-MS was obtained in just over one hour. This long acquisition time is determined by the slow scanning rate of the quadrupole. The same information could be obtained in just over one minute when a time-of-flight mass detector is used instead.

Spectral data at each CV in multiple ion monitoring (MID) are limited to ion intensities of selected species (up to 8 ions) but CV scans for selected ions are quick. The selected ion CV spectrum of the *m/z* 530 ion (Figure 2a) was obtained in single ion monitoring (SIM) in 30 seconds using a 200 ms dwell time. This spectrum shows the CV distribution of the ammonium ion complex $[MNH_4]^+$ of the disaccharide **1**. The CV spectrum of $[MNH_4]^+$ displays one CV peak for this disaccharide complex. The width of this CV peak at half height ($\sim$0.4

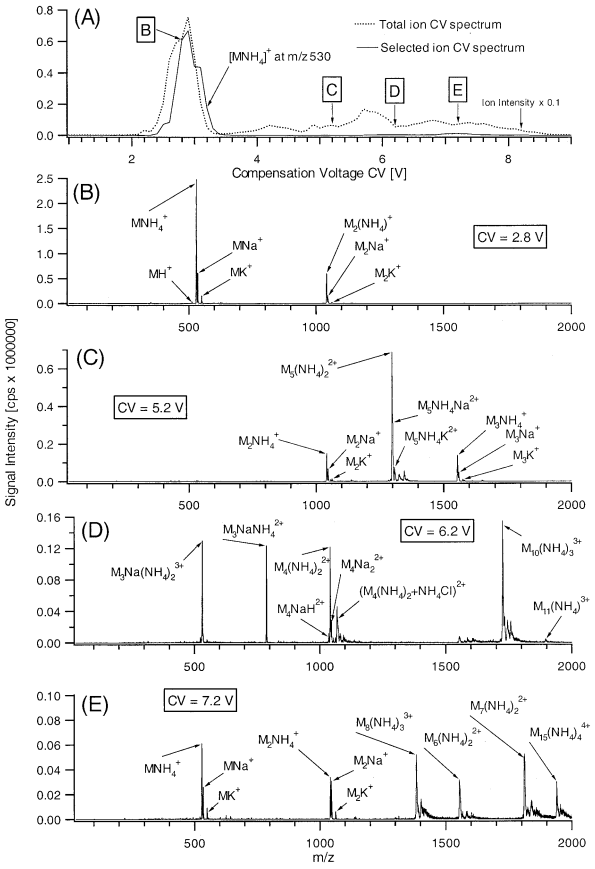


**Figure 2**. Spectra of ions originating from β-D-Glc(1-2)β-D-GalOR at 1 μM concentration in methanol/water (9/1 vol/vol) with 0.2 mM ammonium acetate in positive mode of ESI. FAIMS-MS conditions: Nitrogen gas flow 3 L/min, DV −3.7 kV, spacing between the inner and outer electrode in the spherical part of the FAIMS analyzer 2.3 mm, orifice voltage 0 V, ring electrode voltage 0 V. (**a**) Total ion CV spectrum and selected ion CV spectrum of $[MNH_4]^+$. (**b**) Mass spectrum at CV 2.8 V (5 scans). (**c**) Mass spectrum at CV 5.2 V (5 scans). (**d**) Mass spectrum at CV 6.2 V (5 scans). (**e**) Mass spectrum at CV 7.2 V (5 scans).

V) represents the FAIMS resolution for this disaccharide complex under separation conditions used.

Mass spectra acquired at selected CVs (Figure 2b–e) show that in addition to the most abundant $[MNH_4]^+$ ion other species originating from the disaccharide **1** are detected by FAIMS and that larger complexes are transmitted through the FAIMS at higher CVs. Note that the orifice and the ring electrode of the mass spectrometer were grounded (V = 0) for speciation of disaccharide complexes detected at different CVs. Such conditions in conventional ESI-MS result in total ion loss at the interface and no ion signal for detection. When ions are probed by the mass spectrometer at the same conditions through FAIMS, ion detection is still feasible because of ion focusing properties of this device [39]. Gentle conditions for ion transfer from FAIMS to the quadrupole analyzer are critical in this application because the dissociation of large fragile complex ions that occurs after FAIMS separation at higher ion energy conditions (data not shown) introduces ambiguities in identification of analyzed species. The $[M_5(NH_4)_2]^{2+}$ complex transmitted at CV 5.2 V (Figure 2c), for example, can not be detected at higher ion energies but only its dissociation products including $[M_3NH_4]^+$, $[M_2NH_4]^+$, and $[MNH_4]^+$ are observed. As a result, the $[MNH_4]^+$ would be detected not only at its original transmission CV (2.9 V) but also at CVs where other ions associated with their fragmentation product $[MNH_4]^+$ are transmitted through FAIMS. Low-energy conditions at the mass spectrometer interface help to differentiate ions formed in ESI from their dissociation products.

## *FAIMS Separation of Disaccharide Isomers in Positive Ion Mode*

The diversity of linkage isomers arises from various positions for attachment of a glycosidic linkage whereas the variation of anomers is limited only to the direction of a glycosidic linkage. In positive ESI, these disaccharides form stable complexes with alkali metal ions. Table 2 shows the CV of these complexes for disaccharide anomers **1**, **2** and linkage isomers **3**,**4**. CVs listed in tables correspond to the voltage associated with the maximum of the CV peak. The CV peak width at half height (~0.3 V on average) depends on the identity of the ion. The CV of alkali metal ion complexes with disaccharide anomers increased with the size of the

**Table 2.** Separation of anomers and linkage isomers as positive ions

| | Disaccharide adduct | $H^+$ | $Li^+$ | $NH_4^+$ | $Na^+$ | $K^+$ | $Rb^+$ | $Cs^+$ |
|---|---|---|---|---|---|---|---|---|
| | Anomers | | | Compensation voltage CV [V] | | | | |
| **[1]** | 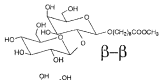 β–β | - | 2.6 | 2.8 | 2.8 | 2.8 | 2.9 | 3.3 |
| **[2]** | 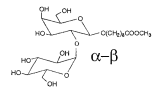 α–β | - | 2.9 | 3.0 | 2.9 | 3.1 | 3.3 | 3.7 |
| | Linkage isomers | | | Compensation voltage CV [V] | | | | |
| **[3]** | 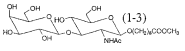 (1-3) | 2.4 | 2.9 | - | 2.6 | 3.1 | 3.4 | 3.8 |
| **[4]** | 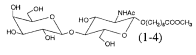 (1-4) | 3.2 | 3.0 | - | 3.2 | 3.2 | 3.6 | 3.9 |

**Table 3.** Separation of position isomers with the amide derivative group as positive ions

| | Disaccharide adduct | $H^+$ | $Li^+$ | $NH_4^+$ | $Na^+$ | $K^+$ | $Rb^+$ | $Cs^+$ |
|---|---|---|---|---|---|---|---|---|
| | 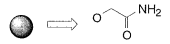 | Compensation voltage CV [V] | | | | | | |
| **[11]** | 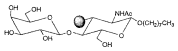 | 2.6 | 3.2 | - | 2.8 | 3.0 | 3.5 | 4.4 |
| **[12]** | 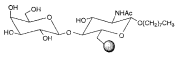 | 3.2 | 3.0 | - | 2.7 | 3.1 | 3.2 | 3.7 |
| **[13]** | 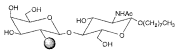 | 3.3 | 3.2 | - | 3.0 | 2.8 | 3.2 | 3.6 |
| **[14]** | 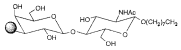 | 4.0 | 2.6 | - | 2.5 | 3.5 | 3.8 | 4.0 |
| **[15]** | 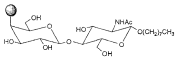 | 2.6 | 2.7 | - | 2.4 | 2.1 | 2.2 | 3.4 |
| **[16]** | 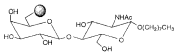 | 2.6 | 2.2 | - | 2.2 | 2.1 | 2.1 | 2.6 |

metal ion involved in complex formation. The CV of the same metal ion complex with different anomers, however, was not the same. Because identical ion complexes of isomers **1** and **2** are transported through FAIMS at different CVs, gas-phase separation of these anomers could be achieved. As can be seen in Table 2, the best separation of anomers **1** and **2** could be expected for rubidium and cesium complexes. Sodium adducts of these isomers, in contrast, were separated only by 0.1 V. Linkage isomers **3** and **4**, as well as position isomers studied, don't form ammonium complexes that could be stable in the gas phase under experimental conditions used; instead, the protonated ions of these disaccharides were observed. The formation of the protonated complexes of disaccharides is facilitated by the presence of a nitrogen atom in the structure of disaccharides. Data in Table 2 show that for linkage isomers **3** and **4**, the CV of a metal ion–disaccharide complex, with the exception of lithium ion, increased with the size of the ion involved in complex formation. The best separation of linkage isomers **3** and **4** was obtained for proton or sodium complexes of these isomers.

Table 3 shows FAIMS separation data of ion complexes with position isomers of $\beta$-D-Gal(1-4)$\beta$-D-GlcNHAcOR. Position isomers of this disaccharide differ by the location of the amide derivative group in the structure of this disaccharide. Separation properties of these complexes depend on the position of the derivative group and the type of ion present in the complex. There is no clear CV dependence on the size of the ion.

Table 4 shows CVs of ion complexes with disaccharides containing different derivitization groups located at the same position. Derivitization groups were chosen to represent similar size. Identical ion complexes of compounds presented in Table 4 have different masses and their mass spectrometry differentiation is trivial. FAIMS separation data of these species indicate, however, that the character of the derivative group provides an important contribution to their separation properties. The structure of the derivative group seems to be more critical than its size.

Figure 3 illustrates FAIMS separation of positively charged metal ion complexes of disaccharide isomers including anomers (Figure 3a), linkage isomers (Figure 3b), and position isomers with the amide derivitization group (Figure 3c). Anomers and position isomers were separated as cesium complexes and linkage isomers were separated as sodium complexes. Anomers and linkage isomers could be separated by FAIMS but CV peaks corresponding to isomer complexes are not baseline-resolved. Separation of all position isomers as cesium complexes could not be achieved. Separation of isomers presented in Figure 3 was accomplished in

**Table 4.** Separation of disaccharides with different different groups as positive ions

| Disaccharide adduct | $H^+$ | $Li^+$ | $NH_4^+$ | $Na^+$ | $K^+$ | $Rb^+$ | $Cs^+$ |
|---|---|---|---|---|---|---|---|
| 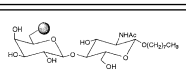 | Compensation voltage CV [V] | | | | | | |
| **[16]** | 2.6 | 2.2 | - | 2.2 | 2.1 | 2.1 | 2.6 |
| **[26]** | 3.2 | 2.5 | - | 2.7 | 3.0 | 3.6 | 4.2 |
| **[36]** | 3.2 | 2.2 | - | 2.6 | 2.7 | 2.9 | 3.2 |
| **[46]** | 2.8 | 2.5 | - | 2.7 | 2.6 | 2.5 | 2.4 |

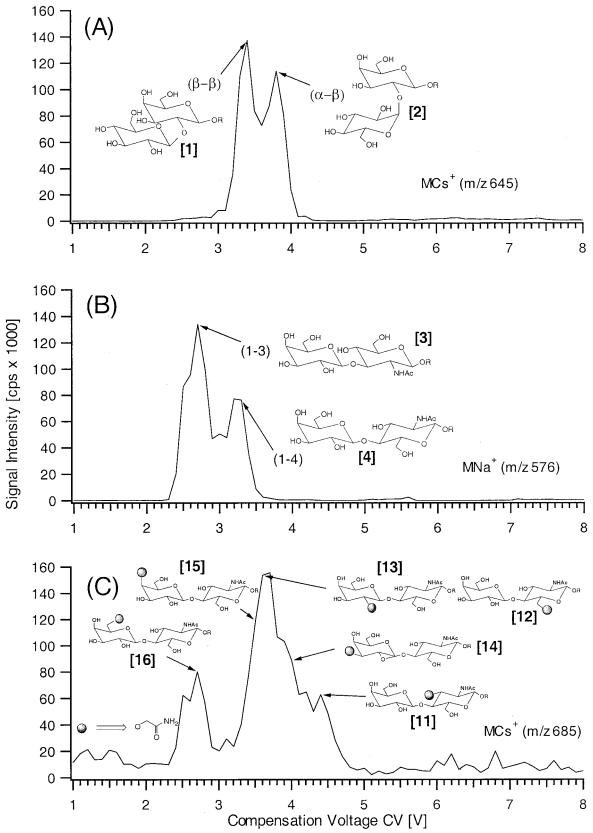


**Figure 3**. FAIMS separation of disaccharide isomers as positive ions. FAIMS-MS conditions: Nitrogen gas flow 3 L/min, DV −3.7 kV, spacing between the inner and outer electrode in the spherical part of the FAIMS analyzer 2.4 mm, orifice voltage 0 V, ring electrode voltage 0 V. (**a**) Disaccharide anomers **1** and **2** at 1 $\mu$M concentration in methanol/water (9/1 vol/vol) with 0.2 mM ammonium acetate and 0.025 mM cesium chloride. (**b**) Linkage isomers **3** and **4** at 1 $\mu$M concentration in methanol/water (9/1 vol/vol) with 0.2 mM ammonium acetate and 0.025 mM sodium chloride. (**c**) Position isomers **11–16** at 1 $\mu$M concentration in methanol/water (9/1 vol/vol) with 0.2 mM ammonium acetate and 0.025 mM cesium chloride.

about 30 seconds. In order to apply this method in analysis of isomers at variable concentrations, baseline resolution of isomers is critical.

## *Separation of Anomers and Linkage Isomers of Disaccharides in Negative Ion Mode*

In negative ESI, disaccharides isomers form deprotonated ions $[M - H]^-$ and a variety of complexes with anions $[M + An^-]^-$ ($An^-$ indicates an anion). Compositional similarities for negative and positive ions formed in ESI include the presence of large and fragile multimer ions. Negative ions, relative to positive ions of comparable size, are transmitted by FAIMS at greater CVs. This feature indicates prospects for better separation of negative ions. At the same time, negative ions seem to be less stable than positive ions. Table 5 shows CVs of negative ions originating from disaccharide anomers **1**, **2** and linkage isomers **3**, **4**. Ions listed in the table include the deprotonated ion of disaccharides $[M - H]^-$ and anion complexes of disaccharides $[M + An^-]$ with chloride ($Cl^-$), acetate ($A^-$), monochloroacetate ($MCA^-$), dichloroacetate ($DCA^-$), trichloroacetate ($TCA^-$), monobromoacetate ($MBA^-$), dibromoacetate ($DBA^-$), tribromoacetate ($TBA^-$), bromochloroacetate ($BCA^-$), chlorodibromoacetate ($CDBA^-$), bromodichloroacetate ($BDCA^-$). Formation of anion complexes of disaccharides is facilitated by addition of anions to disaccharide samples. All presented anion complexes, except a chloride complex, represent fragile species that couldn't be detected using conventional mass spectrometry. The capability of analyzing these fragile ions is important in separation of disaccharide anomers **1** and **2**. The CVs of $[M - H]^-$ and $[M + Cl^-]^-$ for different anomers were identical. Haloacetate complexes of isomers **1** and **2** provided better separation than that for metal ion complexes in positive mode. Linkage isomers **3** and **4**, in contrast, could be separated most efficiently as $[M - H]^-$ and $[M + Cl^-]^-$. The correlation between the CV and the size of an anion present in the complex is different for different isomers. For the disaccharide anomer **2**, CV increases clearly with the size of the anion. For the disaccharide anomer **1** and the linkage isomer **4**, a smaller but opposite trend was observed. There is no such dependence for the linkage isomer **3**.

Figure 4 illustrates separation of disaccharide anomers **1** and **2** as *m/z* 673 trichloroacetate (TCA) com-

**Table 5.** Separation of anomers and linkage isomers as negative ions

| | Disaccharide adduct | $M\text{-}H^-$ | $Cl^-$ | $A^-$ | $MCA^-$ | $DCA^-$ | $TCA^-$ | $MBA^-$ | $DBA^-$ | $TBA^-$ | $BCA^-$ | $CDBA^-$ | $BDCA^-$ |
|---|---|---|---|---|---|---|---|---|---|---|---|---|---|
| | Anomers | | | | | | Compensation voltage CV [V] | | | | | | |
| **[1]** | β–β | 5.6 | 5.7 | 5.6 | 5.8 | 5.7 | 5.7 | 5.8 | 5.6 | 5.5 | 5.7 | 5.5 | 5.6 |
| **[2]** | α–β | 5.6 | 5.7 | 5.8 | 6.4 | 7.0 | 7.8 | 6.5 | 7.3 | 7.9 | 7.2 | 7.9 | 7.8 |
| | Linkage isomers | | | | | | Compensation voltage CV [V] | | | | | | |
| **[3]** | (1-3) | 4.3 | 5.2 | 6.2 | 6.1 | 5.8 | 6.0 | 6.2 | 5.9 | 6.0 | 5.9 | 6.0 | 6.0 |
| **[4]** | (1-4) | 5.7 | 6.4 | 6.8 | 6.8 | 6.3 | 5.8 | 6.7 | 6.1 | 5.6 | 6.2 | 5.6 | 5.7 |

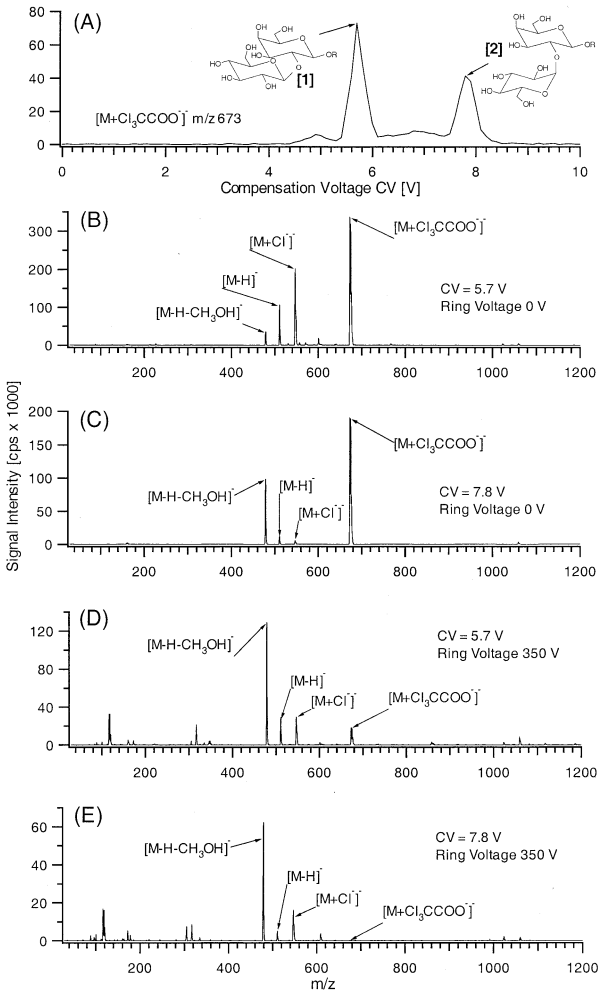


**Figure 4**. Spectra of ions originating from disaccharide anomers **1** and **2** at 1 $\mu$M concentration in methanol/water (9/1 vol/vol) with 0.2 mM ammonium acetate, ammonium hydroxide (0.05%), and 0.025 mM trichloroacetic acid in negative mode ESI. FAIMS-MS conditions: Nitrogen gas flow 4 L/min, DV 3.7 kV, spacing between the inner and outer electrode in the spherical part of the FAIMS analyzer 2.4 mm, orifice voltage 0 V. (**a**) Selected ion CV spectrum of $[M + Cl_3CCOO^-]^-$ at a ring voltage of 0 V. (**b**) Mass spectrum at CV of 5.7 V and a ring voltage of 0 V (5 scans). (**c**) Mass spectrum at CV of 7.8 V and a ring voltage of 0 V (5 scans). (**d**) Mass spectrum at CV of 5.7 V and a ring voltage of 350 V (5 scans). (**e**) Mass spectrum at CV of 7.8 V and a ring voltage of 350 V (5 scans).

plexes. Peaks observed in the CV spectrum (Figure 4a) at 5.7 and 7.8 V correspond to TCA complexes of **1** and **2**, respectively. The mass spectrum acquired at 5.7 V (Figure 4b) shows that in addition to the TCA complex of **1**, $[M + Cl^-]^-$ and $[M - H]^-$ of **1** and **2** (see Table 5) were transmitted through FAIMS at these conditions. The fragmentation product $[M - H - CH_3COOH]^-$ could originate from all ions transmitted at 5.7 V. The mass spectrum acquired at a CV of 7.8 V (Figure 4c) contains an intense peak of the TCA complex of **2**. Because the TCA complex of **2** was the only ion transmitted through FAIMS at 7.8 V, $[M + Cl^-]^-$, $[M - H]^-$, and $[M - H - CH_3OH]^-$ originated from dissociation of the TCA complex of **2**. Spectra in Figure 4a–c were obtained at orifice and ring electrode potentials of 0 V. Mass spectra in Figure 4d and e were acquired at an orifice potential of 0 V and ring electrode potential of −350 V to induce dissociation of ions. As a result, the ion intensity of the TCA complex of **1** (detected at a CV of 5.7 V in Figure 4d) decreased and new dissociation products appeared in the spectrum. The mass spectrum obtained at identical ion energy conditions and a CV of 7.8 V (Figure 4e) indicates total fragmentation of TCA complex of **2**. Direct comparison of dissociation spectra in Figure 4d and e is not possible because fragment ions observed in Figure 4d could originate not only from the TCA complex of **1** but also from other ions. The ring electrode fragmentation under identical CID conditions shows, however, that the TCA complex of **1** (Figure 4d) is more stable than the TCA complex of **2** (Figure 4e). The different stability of these ions should translate to different fragmentation patterns observed in tandem mass spectrometry. Dissociation of TCA complexes occurs at low energy CID conditions. Consequently, these ions are not available for conventional tandem mass spectrometry experiments. Mass spectrometry differentiation of fragile complexes of disaccharide isomers could be evaluated using a combination of FAIMS with tandem mass spectrometry.

Figure 5 illustrates FAIMS separation of linkage isomers **3** and **4** as chloride complexes. The CV spectrum (Figure 5a) of chloride complexes of **3** and **4** shows baseline separation for these isomers analyzed at 1 $\mu$M concentration. The mass spectrum acquired at a CV of 6.3 V (Figure 5b), where the chloride complex of **4** was transmitted through FAIMS, shows that $[M + Cl^-]^-$ is practically the only species observed in the spectrum at 1 $\mu$M concentration. Figure 5c and d show separation and detection capabilities of FAIMS at 10 nM concentrations of linkage isomers **3** and **4** analyzed as chloride complexes. CV peaks of chloride complexes of **3** and **4**, observed in the CV spectrum presented in Figure 5c, are distorted because of chemical noise contribution to the analyte signal. The magnitude of interferences at this concentration level can be observed in the mass spectrum acquired at 6.3 V (Figure 5d). The peak of the chloride complex of the linkage isomer **4** represents only a small fraction of ions transmitted through FAIMS at this CV. The separation and detection of isomers at this concentration is still feasible. Chemical background ions detected in the spectrum shown in Figure 5d determine detection limits in FAIMS. It should be noted that the contribution of interfering ions is greatly reduced by elimination of ions with different ion mobility characteristics during FAIMS separation. A further improvement in detection limits could be achieved by using a high resolution mass spectrometer.

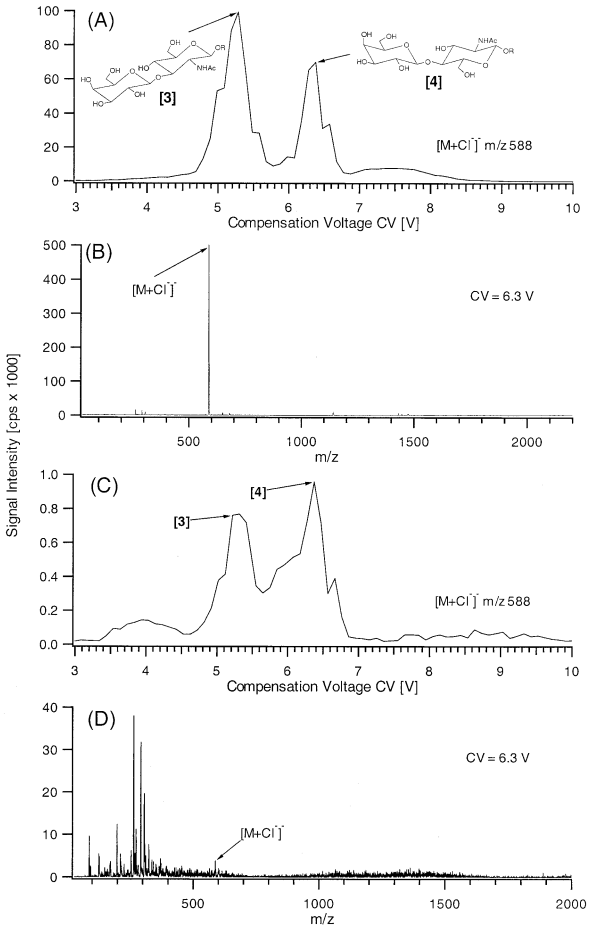


**Figure 5**. Spectra of ions originating from linkage isomers **3** and **4** dissolved in methanol/water (9/1 vol/vol) with 0.2 mM ammonium acetate, ammonium hydroxide (0.05%), and 0.025 mM ammonium chloride in negative mode ESI. FAIMS-MS conditions: Nitrogen gas flow 4 L/min, DV 3.7 kV, spacing between the inner and outer electrode in the spherical part of the FAIMS analyzer 2.4 mm, orifice voltage 0 V, ring voltage 0 V (**a**) Selected ion CV spectrum of $[M + Cl^-]^-$ at 1 $\mu$M concentration of **3** and **4**. (**b**) Mass spectrum at CV 6.3 V and 1 $\mu$M concentration of **3** and **4** (5 scans). (**c**) Selected ion CV spectrum of $[M + Cl^-]^-$ at 10 nM concentration of **3** and **4**. Mass spectrum at CV 6.3 V and 10 nM concentration of **3** and **4** (5 scans).

## *Separation of Position Isomers of Disaccharides in Negative Ion Mode*

Separation properties of negative ions originating from position isomers of the $\beta$-D-Gal(1-4)$\beta$-D-GlcNHAcOR with different derivative groups at different position were investigated by FAIMS. CV data from these experiments for amide **11–16**, carboxylic **21–26**, amine **31–36**, and amidine **41–46** derivative groups are presented in Tables 6, 7, 8, and 9, respectively. There are a few interesting features that relate structural details of ions to the compensation voltage. First, the formation of the anion disaccharide complex changed the CV of the complex relative to the CV of the deprotonated ion of the disaccharide. This CV shift is related to size of the anion involved in complex formation. However, the magnitude of this CV shift depends to a large extent on the location and identity of the derivative group. The CVs of the anion complexes were smaller than the CV of the of the deprotonated ion only when the carboxylic group was located at carbon 2 in the galactose ring **13** and at carbon 4 in the galactose ring **15**. This trend was clearly observed for amide derivatives **23** and **25** and was less pronounced for amine **33** and **35** and amidine **43** and **45** derivatives. Second, multiple peaks were detected in compensation voltage spectra of position isomers. These peaks correspond to different conformers of the complex ion. The tendency for conformer formation depends on the location and identity of the derivative group and also on the identity of the anion involved in complex formation. Among all position isomers, disaccharides with a derivative group located at carbon 6 in the glucose ring **12**, **22**, **32**, **42** and carbon 6 in the galactose ring **36**, **46** form the largest number of conformers. Derivatization groups at these locations are connected to the carbohydrate ring through one additional carbon segment. This arrangement provides conformational flexibility for a derivative group in the formation of intermolecular structures. The number of conformers increased greatly when the derivitization

**Table 6.** Separation of position isomers with the amide derivative group as negative ions

| | Disaccharide adduct | M-H⁻ | Cl⁻ | A⁻ | MCA⁻ | DCA⁻ | TCA⁻ | MBA⁻ | DBA⁻ | TBA⁻ | BCA⁻ | CDBA⁻ | BDCA⁻ |
|---|---|---|---|---|---|---|---|---|---|---|---|---|---|
| | 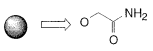 | Compensation voltage CV [V] | | | | | | | | | | | |
| **[11]** | 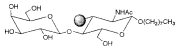 | 3.6 | 4.3 | 3.6 | 4.1 | 4.7 | 4.9 | 4.3 | 4.9 | 5.0 | 4.8 | 5.0 | 5.0 |
| **[12]** | 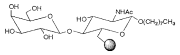 | 4.4 | 5.0 | 4.8 | 5.2 | 5.5 (4.0)* | 5.6 (4.6) | 5.3 | 5.6 | 5.7 | 5.3 | 5.7 | 5.6 (4.6) |
| **[13]** | 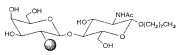 | 4.6 | 3.8 | 4.7 | 4.5 | 4.1 | 4.0 | 4.4 | 4.0 | 3.9 | 4.1 | 3.9 | 3.9 |
| **[14]** | 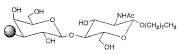 | 3.4 | 4.6 | 4.6 | 4.5 | 4.4 | 4.6 | 4.5 | 4.6 | 4.9 | 4.5 | 4.8 | 4.7 |
| **[15]** | 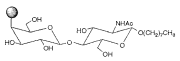 | 5.2 | 4.6 | 4.7 | 4.6 | 4.5 | 4.2 | 4.6 | 4.4 | 4.2 | 4.5 | 4.2 | 4.2 |
| **[16]** | 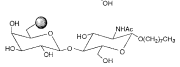 | 3.8 | 4.4 | 4.2 | 4.5 | 4.6 | 4.9 | 4.6 | 4.7 | 5.0 | 4.7 | 5.0 | 5.0 |

*(X.X) denotes that the conformer peak detected at CV of X.X V is smaller than 30% of the major conformer peak.

**Table 7.** Separation of position isomers with the carboxylic derivative group as negative ions

| | Disaccharide adduct | M-H$^-$ | Cl$^-$ | A$^-$ | MCA$^-$ | DCA$^-$ | TCA$^-$ | MBA$^-$ | DBA$^-$ | TBA$^-$ | BCA$^-$ | CDBA$^-$ | BDCA$^-$ |
|---|---|---|---|---|---|---|---|---|---|---|---|---|---|
| | 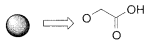 | Compensation voltage CV [V] | | | | | | | | | | | |
| **[21]** | 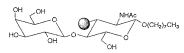 | 3.7 | 3.6 | 4.1 | 3.5 | 3.7 | 4.3 | 3.5 | 4.0 | 4.7 | 3.9 | 4.6 | 4.6 |
| **[22]** | 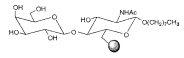 | 4.5 | 5.1 | 5.4 | 5.0<br>(4.7)* | 5.0 | 5.5<br>(4.3) | 5.0 | 4.2<br>(5.3) | 3.8<br>(5.6) | 5.1<br>(3.6) | 3.8<br>(5.5) | 5.5<br>(4.1) |
| **[23]** | 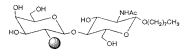 | 6.0 | 3.6 | 4.1 | 4.0 | 3.9 | 3.9 | 4.0 | 4.0 | 3.9 | 4.0 | 3.9 | 3.9 |
| **[24]** | 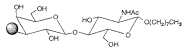 | 9.2<br>(4.4) | 7.2<br>(4.1) | 7.1<br>(4.2) | 4.4 | 4.5 | 4.6 | 4.4 | 4.5 | 5.2 | 4.5 | 4.8 | 4.7 |
| **[25]** | 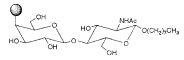 | 4.5 | 4.3 | 4.2 | 4.2 | 4.4 | 4.3 | 4.2 | 4.3 | 4.4 | 4.4 | 4.4 | 4.4 |
| **[26]** | 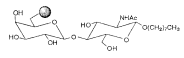 | 3.5 | 3.8 | 3.8 | 4.1 | 4.5 | 5.0 | 4.1 | 4.7 | 5.0 | 4.7 | 5.0 | 4.9 |

*(X.X) denotes that the conformer peak detected at CV of X.X V is smaller than 30% of the major conformer peak.

group did not carry charge. These observations suggest that intermolecular interaction in the complex could change its structure and be responsible for formation of conformers. Anion complexes of disaccharides represent a larger variety of structures than metal ion complexes of disaccharides examined in positive ion mode (Table 4).

There are also some limitations in analysis of position isomers as negative ions. Amine (Table 8) or amidine (Table 9) derivatives of disaccharides showed low ionization efficiency in negative mode ESI. Although negative species of these derivatives could be examined by FAIMS, analyses of these compounds at low concentrations would be recommended in positive ion mode. Tabulated data for position isomers of disaccharides can be used to design a quick method for differentiation of these isomers. Differentiation of position isomers with the carboxylic group is illustrated in Figure 6. When a mixture of six position isomers **21**–**26** was analyzed as deprotonated ions (Figure 6a), only two isomers, **23** and **24**, were separated. There is an overlap for two other pairs of position isomers. The deprotonated ion of **24** shows two conformers. The major one is separated at 9.2 V and minor one (20% intensity of the major conformer) is separated at 4.4 V. To separate overlapping species, isomers **22**, **24**, and **25** should be analyzed as chloride complexes (Figure 6b) and isomers **21** and **26** should be analyzed as trichloroacetate complexes (Figure 6c). Separation of disaccharide isomers presented in Figures 5, 6, and 7 was accomplished in about 30 seconds.

## *Comparison of FAIMS with Ion Mobility Spectrometry*

The FAIMS separation of two trisaccharide isomers (melezitoze and raffinoze) is illustrated by selected ion CV spectra of raffinoze (Figure 7a), melezitoze (Figure 7b), and a mixture of both isomers (Figure 7c). These isomers have different sequence, linkage, and anomeric configuration but have the same molecular mass. Me-

**Table 8.** Separation of position isomers with the amine derivative group as negative ions

| | Disaccharide adduct | M-H$^-$ | Cl$^-$ | A$^-$ | MCA$^-$ | DCA$^-$ | TCA$^-$ | MBA$^-$ | DBA$^-$ | TBA$^-$ | BCA$^-$ | CDBA$^-$ | BDCA$^-$ |
|---|---|---|---|---|---|---|---|---|---|---|---|---|---|
| | 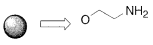 | Compensation voltage CV [V] | | | | | | | | | | | |
| **[41]** | 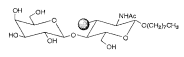 | 5.0 | 4.8 | 4.5 | 4.6 | 4.1<br>(4.7)* | 4.1<br>(4.7) | 4.7 | 4.7<br>(4.1) | 4.2<br>(4.8) | 4.7<br>(4.1) | 4.2<br>(4.8) | 4.1<br>(4.7) |
| **[42]** | 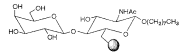 | 5.0 | 4.9 | 4.6 | 5.0 | 5.1<br>(4.0) | 5.5<br>(4.0) | 5.0 | 5.4<br>(4.1) | 5.6<br>(4.0) | 5.3<br>(4.0) | 5.6<br>(4.0) | 5.5<br>(4.0) |
| **[43]** | 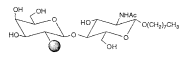 | 5.2 | 3.8 | 3.6<br>(4.9) | 5.0 | 4.6 | 5.0<br>(5.6) | 4.3 | 4.8<br>(5.7) | 5.4 | 4.7 | 5.3 | 5.0<br>(5.6) |
| **[44]** | 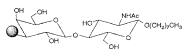 | 4.9 | 4.6 | 5.0 | 4.7<br>(3.9) | 4.7 | 4.8 | 4.6 | 4.8 | 4.8 | 4.8 | 4.8 | 4.8 |
| **[45]** | 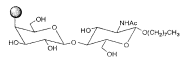 | 4.8 | 4.8 | 4.9 | 5.3<br>(4.4) | 5.3 | 4.9 | 5.3 | 5.1 | 4.8<br>(6.2) | 5.0 | 4.8<br>(6.2) | 4.9 |
| **[46]** | 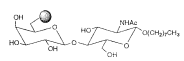 | 4.6<br>(7.3) | 4.6<br>(3.9) | 4.5 | 3.6<br>(5.9) | 6.0 | 4.6<br>(7.3) | 6.0 | 4.6<br>(7.0) | 4.6<br>(7.3) | 4.6<br>(6.8) | 4.6<br>(7.3) | 4.6<br>(7.3) |

*(X.X) denotes that the conformer peak detected at CV of X.X V is smaller than 30% of the major conformer peak.

**Table 9.** Separation of position isomers with the amidine derivative group as negative ions

| | Disaccharide adduct | M-H$^-$ | Cl$^-$ | A$^-$ | MCA$^-$ | DCA$^-$ | TCA$^-$ | MBA$^-$ | DBA$^-$ | TBA$^-$ | BCA$^-$ | CDBA$^-$ | BDCA$^-$ |
|---|---|---|---|---|---|---|---|---|---|---|---|---|---|
| | 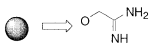 | Compensation voltage CV [V] | | | | | | | | | | | |
| **[31]** | 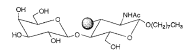 | 4.5 | 4.8 | 4.7 | 5.1 | 3.8 | 4.0 | 5.2 | 4.0 | 4.2 | 3.8 | 4.0 | 4.0 |
| | | (5.0)* | (3.8) | | (3.6) | (5.1) | (5.0) | (3.7) | (5.0) | (4.9) | (5.1) | (5.0) | (5.0) |
| **[32]** | 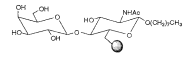 | 4.5 | 4.7 | 4.1 | 4.3 | 4.3 | 4.5 | 4.3 | 4.5 | 4.6 | 4.5 | 4.6 | 4.6 |
| | | (5.5) | | (5.0) | | (4.8) | (5.0) | (5.6) | (5.0) | 5.5 | (5.0) | (5.1) | (5.1) |
| **[33]** | 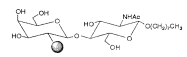 | 4.2 | 3.9 | 4.8 | 4.9 | 4.5 | 4.3 | 4.9 | 4.5 | 4.2 | 4.4 | 4.2 | 4.3 |
| | | 5.0 | 5.0 | | | 5.3 | 5.0 | | (5.3) | 5.6 | 5.2 | (5.1) | 5.0 |
| | | (5.9) | (6.7) | | | | 5.7 | | | | | | 5.7 |
| **[34]** |  | 4.0 | 4.6 | 4.3 | 4.6 | 4.6 | 4.5 | 4.6 | 4.6 | 4.5 | 4.6 | 4.5 | 4.6 |
| | | (4.6) | | | | (5.1) | | | (5.5) | | (5.1) | (5.5) | |
| **[35]** | 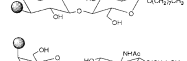 | 4.3 | 4.3 | 4.5 | 4.5 | 4.7 | 4.5 | 4.6 | 4.7 | 4.2 | 4.7 | 5.5 | 4.4 |
| | | 4.8 | | (5.5) | (5.5) | (5.6) | (5.5) | (5.3) | (5.6) | (5.3) | (5.6) | (4.2) | (5.5) |
| | | 5.6 | | | | | | | | | | | |
| **[36]** | 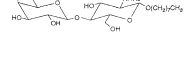 | 3.8 | 4.4 | 4.3 | 4.9 | 4.2 | 4.3 | 5.0 | 4.5 | 4.5 | 4.2 | 4.4 | 4.3 |
| | | | (3.1) | | | 4.9 | (5.4) | | (5.4) | (5.3) | 5.0 | (5.4) | (5.4) |

*(X.X) denotes that the conformer peak detected at CV of X.X V is smaller than 30% of the major conformer peak.

lezitoze and raffinoze have been analyzed previously using ion mobility spectrometry (IMS) [33], where the difference in ion mobilities at a low electric field provides the prerequisite for ion separation. Raffinose and melezitoze isomers were separated in IMS as deprotonated ions in nitrogen gas, so the same species with the same buffer gas were examined in FAIMS to obtain fair comparison of different ion mobility separation methods. The FAIMS separation of deprotonated isomer ions was accomplished based on a difference in their relative mobilities at high and low electric field. The resolution of these species obtained in FAIMS (calculated as the difference in compensation voltages divided by the average of compensation voltages) equals 0.080. The separation of identical ions in Ion Mobility Spectrometry resulted in overlapping of two isomer peaks in the ion mobility distribution spectrum. In fact, the difference in arriving times of isomer ions (2.162 ms and 2.135 ms) was only slightly larger than experimental uncertainties. The resolution of these isomers in IMS (calculated as the difference in arriving times divided by the average of arriving times) equals 0.013. Assuming that the ion mobility of examined isomer ions at low field is approximately the same, the high-field ion mobility of these two ions contributes greatly to the resolving power of FAIMS.

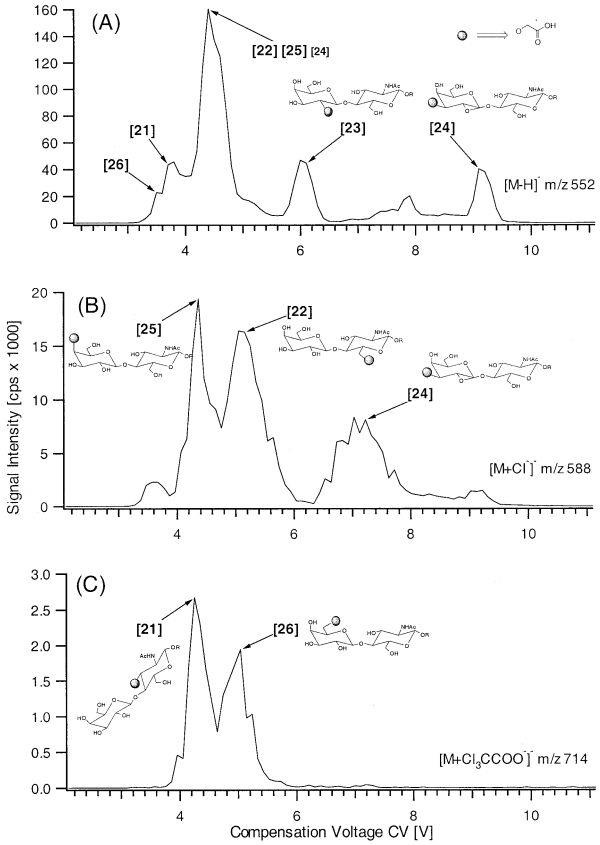


**Figure 6.** FAIMS separation of position isomers of disaccharides as negative ions. FAIMS-MS conditions: Nitrogen gas flow 4 L/min, DV 3.7 kV, spacing between the inner and outer electrode in the spherical part of the FAIMS analyzer 2.4 mm, orifice voltage 0 V, ring voltage 0 V (**a**) Selected ion CV spectrum of $[M - H]^-$ at 1 $\mu$M concentration of **21**–**26** in methanol/water (9/1 vol/vol) with 0.2 mM ammonium acetate, ammonium hydroxide (0.05%). (**b**) Selected ion CV spectrum of $[M - Cl^-]^-$ at 1 $\mu$M concentration of **22**, **24**, and **25** in methanol/water (9/1 vol/vol) with 0.2 mM ammonium acetate, ammonium hydroxide (0.05%), and 0.025 mM ammonium chloride. (**c**) Selected ion CV spectrum of $[M + Cl_3CCOO^-]^-$ at 1 $\mu$M concentration of **21** and **26** in methanol/water (9/1 vol/vol) with 0.2 mM ammonium acetate, ammonium hydroxide (0.05%), and 0.025 mM trichloroacetic acid.

## *Considerations Related to the Separation Mechanism of Disaccharide Ions in FAIMS*

A theoretical treatment of FAIMS should include a combination of high and low electric field ion mobilities. The evaluation of ion mobilities at low electric field [40] and comparison of the theoretical values with experimental data is good. At high electric fields, the ion energy is much greater than the thermal energy of the neutral gas molecules. This feature hampered the application of classical theory to describe ion mobility

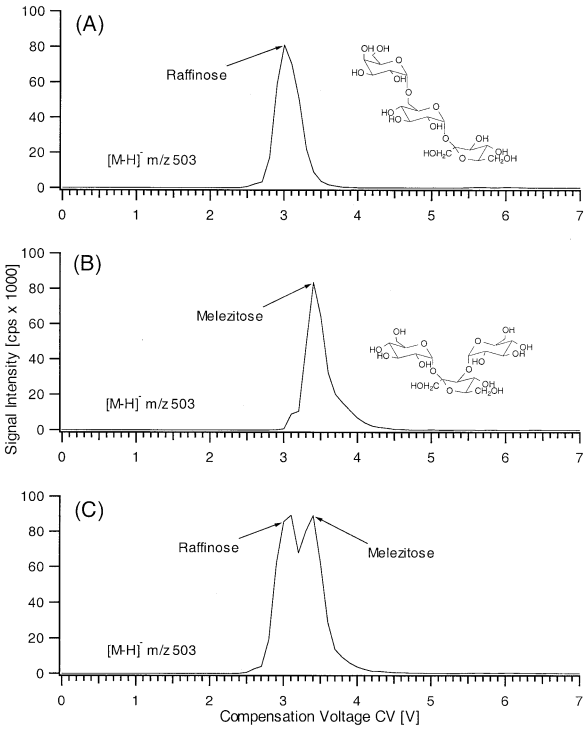


**Figure 7**. CV spectra of raffinose and melezitose at 1 $\mu$M concentration in methanol/water (9/1 vol/vol) with 0.2 mM ammonium acetate, ammonium hydroxide (0.05%) in negative mode of ESI. FAIMS-MS conditions: Nitrogen gas flow 4 L/min, DV 3.7 kV, spacing between the inner and outer electrode in the spherical part of the FAIMS analyzer 2.4 mm, orifice voltage 0 V, ring voltage 0 V. (**a**) Selected ion CV spectrum of $[M - H]^-$ for raffinose. (**b**) Selected ion CV spectrum of $[M - H]^-$ for melezitose. (**c**) Selected ion CV spectrum of $[M - H]^-$ for raffinose and melezitose.

in a high field. The first successful "two-temperature" theory [41] has been accommodated also to evaluate high-field ion mobilities obtained by FAIMS [42]. The agreement between theoretical prediction and experimental results from FAIMS was found for the monoatomic cesium ion and gases of oxygen and nitrogen. However, considerable discrepancy was observed for carbon dioxide. It is clear that the "two temperature" theory with its limitations could not be successfully applied to more complex disaccharide ions displaying a large number of degrees of freedom.

There are important observations from FAIMS separation of disaccharide isomers that should be considered in a model describing separation mechanism of these ions. First, the structure and charge distribution of ions determine their separation properties in FAIMS. For example, the presence of a polar derivative group at a specific location was shown to influence the structure and charge distribution of position isomers that could be translated directly to CVs obtained in FAIMS separation. Second, the difference in mobilities at high and low electric field for disaccharide ions was observed only above a certain electric field strength threshold. The threshold values depend on the identity of ions but in general are close to 10,000 V/cm (DV = 2.0 kV). It should be pointed out that such electric field strengths are at least two orders of magnitude greater than those used in drift tube experiments, where ion mobilities at high fields were studied previously.

The fact that FAIMS separation based on the *relative* ion mobility could be achieved only above a certain electric field threshold indicates that in addition to collision effects there are other important factors affecting high-field mobility of disaccharide ions. Note that if the *relative* ion mobility were affected only by the collision process, one would expect to see these variations also at field strengths smaller than −10,000 V/cm. A logical explanation for this observation is the orientation of disaccharide ions under the influence of high electric field. A theoretical assumption from drift tube experiments [41, 43, 44], i.e., that moving ions experience free rotation ("tumbling"), is not necessarily valid at much stronger electric fields used in FAIMS. Interactions between disaccharide ions and the applied high electric field not only provide kinetic energy to ions moving between electrodes but also could force the energetically most favorable orientation of these ions in the electric field. This orientation would depend on the direction of the dipole moment of the ion that exists or is induced at a particular field. The orientation force would depend on the magnitude of the dipole moment and the electric field strength. Ion–gas collisions would try to restore random orientation of the ion and contribute to changes in the ion orientation from that determined by high electric field.

The electric field applied in FAIMS changes continuously with a frequency of 750 kHz according to the shape of the asymmetric waveform [35]. This means that ions experience a high-field force only for a small fraction of a microsecond. After that, for a little more than 1$\mu$s, the electric field decreases, assumes opposite polarity, and increases slightly in order to reach the maximum value again. The duration of the polarity change in the applied field is less than 1$\mu$s. In this short period, the disaccharide ion doesn't have enough time to change its orientation by rotation. Note that rotational frequencies of disaccharide ions are a few times smaller than the frequency of the asymmetric waveform. As a result, the disaccharide ion in the low electric field of opposite polarity could depart only slightly from the orientation determined earlier by the high electric field. It should be noted that the changes in the ion orientation and resulting changes in the collision cross-section would fluctuate continuously in each cycle of the asymmetric waveform.

All aspects of ion–gas collisions (the ion–gas interaction potential, elastic and inelastic collisions) are still essential in the proposed model but the collision process must be considered for ions that could accommodate an orientation established by a high electric field. FAIMS data for disaccharide isomers support assumptions made in the proposed model. The high-field mobility of all disaccharide ions studied is smaller than their mobility at low field. The direction of the dipole

moment for these ions is approximately perpendicular to the main axis of the structural skeleton. Orientation of these ions in such a way that the direction of the dipole moment is parallel to the direction of electric field causes the collision cross-section of "frozen" ions (high field) to be larger than the collision cross-section of ions that depart slightly (low field) from this orientation. The evaluation of the model for FAIMS separation of disaccharide ions, based on their structure and charge distribution from molecular modeling, will be presented in a separate publication.

## Conclusions

Requirements and capabilities of FAIMS-MS for the analysis of disaccharide isomers were demonstrated in this work. In addition to isomer separation, this technique offers high speed and high sensitivity of detection relative to conventional methods. The separation of structurally similar species was accomplished by analyzing ions that are not observed in conventional mass spectrometry. FAIMS-MS was shown to have a unique ability to preserve and monitor fragile ion complexes formed in electrospray.

FAIMS as a continuous separation method is especially useful in characterization of ions. Species separated at a particular CV are available for MS analysis as long as the ionization method provides a continuous stream of ions. In contrast to liquid separation methods, the ion availability in FAIMS is not restricted by time (a peak width in liquid separation methods) or low intensities of examined ions. The investigation of separated ions could be carried out collecting and averaging a large number of spectra.

Presented data for disaccharide isomers provide information to gain better understanding of FAIMS separation. Separation conditions for disaccharide isomers used in our experiments could be still improved. Preliminary experiments showed that use of an asymmetric waveform with DV greater than 3.7 kV provides better separation for isomers. Another factor that could improve separation of isomers is the type of buffer gas used in FAIMS separation. Using helium instead of nitrogen could extend the CV range at which disaccharide ions are detected and provide better separation between isomers. These modifications will be considered when this method is applied to larger group of carbohydrates.

## References


1. Bjorndal, H.; Lindberg, B.; Svensson, S. Mass Spectrometry of Partially Methylated Alditol Acetates. *Carbohydr. Res.* **1967,** *5,* 433–440.
2. Aspinall, G. O. *The Polysaccharides;* Academic Press: New York, 1982; Vol. I. 1984; Vol. II. 1985; Vol. III.
3. Wang, W. T.; LeDonne, N. C.; Ackerman, B., Jr.; Sweeley, C. C. Structural Characterization of Oligosaccharides by High Performance Liquid Chromatography, Fast Atom Bombardment Mass Spectrometry, and Exoglycosidase Digestion. *Anal. Biochem.* **1984,** *141,* 366–381.
4. Her, G. R.; Santikarn, S.; Reinhold, V. N.; Williams, J. C. Simplified Approach to HPLC Precolumn Fluorescent Labeling of Carbohydrates—N-(2-Pyridinyl)-Glycosylamines. *J. Carbohydr. Chem.* **1987,** *6,* 129–139.
5. Gillece-Castro, B. L.; Fisher, S. J.; Tarentino, A. L.; Peterson, D. L.; Burlingame, A. L. Structure of the Oligosaccharide Portion of Human Hepatitis-B Surface Antigen. *Arch. Biochem. Biophys.* **1987,** *256,* 194–201.
6. Poulter, L.; Burlingame, A. L.; McCloskey, J. A. Desorption Mass Spectrometry of Oligosaccharides Coupled with Hydrophobic Chromophores. In *Methods in Enzymology*; Vol. CXCII. Academic Press: San Diego, 1990; p 661.
7. Li, D. T.; Her, G. R. Structural Analysis of Chromophore-Labeled Disaccharides and Oligosaccharides by Electrospray Ionization Mass Spectrometry and High Performance Liquid Chromatography/Electrospray Ionization Mass Spectrometry. *J. Mass Spectrom.* **1998,** *33,* 644–652.
8. Dell, A.; Oates, J. E.; Morris, H. R.; Egge, H. Structure Determination of Carbohydrates and Glycosphingolipids by Fast Atom Bombardment Mass Spectrometry. *Int. J. Mass Spectrom. Ion Processes* **1983,** *46,* 415–418.
9. Northnagel, E. A.; McNeil, M.; Albersheim, P.; Dell, A. Host–Pathogen Interactions. Paper no. 22. A Galacturonic Acid Oligosaccharide from Plant Cell Walls Elicits Phytoalexins. *Plant Physiol.* **1983,** *71,* 916–926.
10. Chai, W.; Cashmore, G. C.; Stoll, M. S.; Gaskell, S. J.; Orkiszewski, R. S.; Lawson, A. M. Oligosaccharide Sequence Determination Using B/E Linked Field Scanning or Tandem Mass Spectrometry of Phosphotidylethanolamine Derivatives. *Biol. Mass Spectrom.* **1991,** *20,* 313–323.
11. Kuster, B.; Naven, T. J. P.; Harvey, D. J. Rapid Approach for Sequencing Neutral Oligosaccharides by Exoglycosidase Digestion and Matrix-Assisted Laser Desorption Ionization Time-of-Flight Mass Spectrometry. *J. Mass Spectrom.* **1996,** *31,* 1131–1140.
12. Garozzo, D.; Giuffrida, M.; Impallomeni, G.; Ballistreri, A.; Montuado, G. Determination of Linkage Position and Identification of the Reducing End in Linear Oligosaccharides by Negative Ion Fast Atom Bombardment Mass Spectrometry. *Anal. Chem.* **1990,** *62,* 279–286.
13. Dell, A.; Taylor, G. W. High-Field-Magnet Mass Spectrometry of Biological Molecules. *Mass Spectrom. Rev.* **1984,** *3,* 357–394.
14. Domon, B.; Costello, C. E. Structure Elucidation of Glycosphingolipids and Gangliosides Using High Performance Tandem Mass Spectrometry. *Biochemistry* **1988,** *27,* 1534–1543.
15. Dallinga, J. W.; Heerma, W. Reaction Mechanism and Fragment Ion Structure Determination of Deprotonated Small Oligosaccharides, Studied by Negative Ion Fast Atom Bombardment (tandem) Mass Spectrometry. *Biol. Mass Spectrom.* **1991,** *20,* 215–231.
16. Hofmeister, G. E.; Zhou, Z.; Leary, J. A. Linkage Position Determination in Lithium-Cationized Disaccharides—Tandem Mass Spectrometry and Semiempirical Calculations. *J. Am. Chem. Soc.* **1991,** *113,* 5964–5970.
17. Ngoka, L. C.; Gall, J. F.; Lebrilla, C. B. Effects of Cations and Charge Types on the Metastable Decay Rates of Oligosaccharides. *Anal. Chem.* **1994,** *66,* 692–698.
18. Carroll, J. A.; Ngoka, L. C.; Beggs, C. G.; Lebrilla, C. B. Liquid Secondary Ion Mass Spectrometry Fourier Transform Mass Spectrometry of Oligosaccharide Anions. *Anal. Chem.* **1993,** *65,* 1582–1587.
19. Mock, K. K.; Davey, M.; Cottrell, J. S. The Analysis of Underivatised Oligosaccharides by Matrix-Assisted Laser Desorption Mass Spectrometry. *Biochem. Biophys. Res. Commun.* **1991,** *177,* 644–651.

20. Mock, K. K.; Sutton, C. W.; Cottrell, J. S. Sample Immobilization Protocols for Matrix-Assisted Laser Desorption Mass Spectrometry. *Rapid Commun. Mass Spectrom.* **1992,** *6,* 233–238.
21. Stahl, B.; Steup, M.; Karas, M.; Hillenkamp, F. Analysis of Neutral Oligosaccharides by Matrix-Assisted Laser Desorption Ionization Mass Spectrometry. *Anal. Chem.* **1991,** *63,* 1463–1466.
22. Harvey, D. J.; Rudd, P. M.; Bateman, R. H.; Bordoli, R. S.; Howes, K.; Hoyes, J. B.; Vickers, R. G. Examination of Complex Oligosaccharides by Matrix-Assisted Laser Desorption Ionization Mass Spectrometry on Time-of-Flight and Magnetic Sector Instruments. *Org. Mass. Spectrom.* **1994,** *29,* 753–766.
23. Spengler, B.; Kirsch, D.; Kaufmann, R.; Lemoine, J. Structure-Analysis of Branched Oligosaccharides Using Post-Source Decay in Matrix-Assisted Laser Desorption Ionization Mass Spectrometry. *Org. Mass Spectrom.* **1994,** *29,* 782–787.
24. Ohashi, Y. Electrospray Ionization Mass Spectrometry of Carbohydrates and Lipids. In *Electrospray Ionization Mass Spectrometry: Fundamentals, Instrumentation, and Applications*; Cole, R. B., Ed.; John Wiley and Sons, Inc.: New York, 1997; p 459.
25. Mulroney, B.; Traeger, J. C.; Stone, B. A. Determination of Both linkage Position and Anomeric Configuration in Underivatized Glucopyranosyl Disaccharides by Electrospray Mass Spectrometry. *J. Mass Spectrom.* **1995,** *30,* 1277–1283.
26. Fura, A.; Leary, J. A. Differentiation of Ca2+-Coordinated and Mg2+-Coordinated Branched Trisaccharide Isomers—An Electrospray Ionization and Tandem Mass Spectrometry Study. *Anal. Chem.* **1993,** *65,* 2805–2811.
27. Garozzo, D.; Impallomeni, G.; Spina, E.; Green, B. N.; Hutton, T. Linkage Analysis in Disaccharides by Electrospray Mass Spectrometry. *Carbohydr. Res.* **1991,** *221,* 253–257.
28. Domon, B.; Muller, D. R.; Richter, W. J. Identification of Interglycosidic Linkages and Sugar Constituents in Disaccharide Subunits of Larger Glycosides by Tandem Mass Spectrometry. *Org. Mass Spectrom.* **1989,** *24,* 357–359.
29. Laine, R. A.; Pamidimukkala, K. M.; French, A. D.; Hall, R. W.; Abbas, S. A.; Jain, R. K.; Matta, K. L. Linkage Position in Oligosaccharides by Fast Atom Bombardment Ionization Collision-Activated Dissociation Tandem Mass Spectrometry and Molecular Modeling. *J. Am. Chem. Soc.* **1988,** *110,* 6931–6939.
30. Smith, G.; Leary, J. A. Differentiation of Stereochemistry of Glycosidic Bond Configuration: Tandem Mass Spectrometry of Diastereomeric Cobalt–Glucosyl–Glucose Disaccharide Complexes. *J. Am. Soc. Mass Spectrom.* **1996,** *7,* 953–957.
31. Zhu, J. H.; Cole, R. B. Ranking of Gas-Phase Acidities and Chloride Affinities of Monosaccharides and Linkage Specificity in Collision-Induced Decompositions of Negative Ion Electrospray-Generated Chloride Adducts of Oligosaccharides. *J. Am. Soc. Mass Spectrom.* **2001,** *12,* 1193–1204.
32. Srebalus, C. A.; Hilderbrand, A. E.; Valentine, S. J.; Clemmer, D. E. Resolving Isomeric Peptide Mixtures: A Combined HPLC/Ion Mobility-TOFMS Analysis of a 4000-Component Combinatorial Library. *Anal. Chem.* **2002,** *74,* 26–36.
33. Liu, Y. S.; Clemmer, D. E. Characterizing Oligosaccharides Using Injected-Ion Mobility Mass Spectrometry. *Anal. Chem.* **1997,** *69,* 2504–2509.
34. Leavell, M. D.; Gaucher, S. P.; Taraszka, J. A.; Clemmer, D. A.; Leary, J. A. Ion Mobility Measurements of Metal-Ligated Monosaccharides Diastereomers. *Procedings of the 48th ASMS Conference on Mass Spectrometry and Allied Topics*; Palm Beach, CA, May, 2000; p 1342–1343.
35. Guevremont, R.; Barnett, D. A.; Purves, R. W.; Vandermey, J. Analysis of a Tryptic Digest of Pig Hemoglobin Using ESI-FAIMS-MS. *Anal. Chem.* **2000,** *72,* 4577–4584.
36. Viehland, L. A.; Guevremont, R.; Purves, R. W.; Barnett, D. A. Comparison of High-Field Ion Mobility from Drift Tubes and a FAIMS Apparatus. *Int. J. Mass Spectrom.* **2000,** *197,* 123–130.
37. Buryakov, I. A.; Krylov, E. V.; Nazarov, E. G.; Rasulev, U. K. A New Method of Separation of Multi-Atomic Ions by Mobility at Atmospheric Pressure Using a High-Frequency Amplitude-Asymmetric Strong Electric Field. *Int. J. Mass Spectrom. Ion Processes* **1993,** *128,* 143–148.
38. Purves, R. W.; Guevremont, R. Electrospray Ionization High-Field Asymmetric Waveform Ion Mobility Spectrometry-Mass Spectrometry. *Anal. Chem.* **1999,** *71,* 2346–2357.
39. Guevremont, R.; Purves, R. W. Atmospheric Pressure Ion Focusing in a High-Field Asymmetric Waveform Ion Mobility Spectrometer. *Rev. Sci. Instrum.* **1999,** *70,* 1370–1383.
40. Clemmer, D. E.; Jarrold, M. F. Ion Mobility Measurements and Their Applications to Clusters and Biomolecules. *J. Mass Spectrom.* **1997,** *32,* 577–592.
41. Viehland, L. A.; Mason, E. A. Gaseous Ion Mobility in Electric Fields of Arbitrary Strength. *Annu. Phys.* **1975,** *91,* 499–533.
42. Barnett, D. A.; Ells, B.; Guevremont, R.; Purves, R. W.; Viehland, L. A. Evaluation of Carrier Gases for Use in High-Field Asymmetric Waveform Ion Mobility Spectrometry. *J. Am. Soc. Mass Spectrom.* **2000,** *11,* 1125–1133.
43. Lin, S. L.; Viehland, L. A.; Mason, E. A. 3-Temperature Theory of Gaseous Ion Transport. *Chem. Phys.* **1979,** *37,* 411–424.
44. Viehland, L. A.; Lin, S. L.; Mason, E. A. Kinetic Theory of Drift Tube Experiments with Polyatomic Species. *Chem. Phys.* **1981,** *54,* 341–364.